Pursuit of an Electron Deficient Titanium Nitride

Grant, L.N.; Bhunia, M.; Pinter, B.; Rebreyend, C.; Carroll, M.E.; Carroll, P.J.; de Bruin, B.; Mindiola, D.J.

DOI
10.1021/acs.inorgchem.0c03644

Publication date
2021

Document Version
Final published version

Published in
Inorganic Chemistry

Inorganic Chemistry

pubs.acs.org/IC

Article

Pursuit of an Electron Deficient Titanium Nitride

Lauren N. Grant,[$] Mrinal Bhunia,[$] Balazs Pinter,* Christophe Rebreyend, Maria E. Carroll, Patrick J. Carroll, Bas de Bruin, and Daniel J. Mindiola*

Cite This: *Inorg. Chem.* 2021, 60, 5635−5646

Read Online

ACCESS | Metrics & More | Article Recommendations | Supporting Information

ABSTRACT: The nitride salt $[(PN)_2Ti{\equiv}N\{\mu_2\text{-}K(OEt_2)\}]_2$ (**1**) (PN^- = (*N*-(2-P^iPr_2-4-methylphenyl)-2,4,6-$Me_3C_6H_2$) can be oxidized with two equiv of I_2 or four equiv of $ClCPh_3$ to produce the phosphinimide-halide complexes (NPN')(PN)Ti-(X) (X^- = I (**2**), Cl (**3**); NPN' = N-(2-NP^iPr_2-4-methylphenyl)-2,4,6-$Me_3C_6H_2^{2-}$), respectively. In the case of **2**, H_2 was found to be one of the other products; whereas, $HCPh_3$ and Gomberg's dimer were observed upon the formation of **3**. Independent studies suggest that the oxidation of **1** could imply the formation of the transient nitridyl species $[(PN)_2Ti(\equiv N\bullet)]$ (**A**), which can either oxidize the proximal phosphine atom to produce the Ti(III) intermediate [(NPN')(PN)Ti] (**B**) or, alternatively, engage in H atom abstraction to form the parent imido $(PN)_2Ti{\equiv}NH$ (**4**). The latter was independently prepared and was found to photochemically convert to the titanium-hydride, (NPN')(PN)Ti(H) (**5**). Isotopic labeling studies using $(PN)_2Ti{\equiv}ND$ (**4**-d_1) as well as reactivity studies of **5** with a hydride abstractor demonstrate the presence of the hydride ligand in **5**. An alternative route to putative **A** was observed via a photochemically promoted incomplete reduction of the azide ligand in $(PN)_2Ti(N_3)$ (**6**) to **4**. This process was accompanied by some formation of **5**. Frozen matrix X-band EPR studies of **6**, performed under photolytic conditions, were consistent with species **B** being formed under these reaction conditions, originating from a low barrier N-insertion into the phosphine group in the putative nitridyl species **A**. Computational studies were also undertaken to discover the mechanism and plausibility of the divergent pathways (via intermediates **A** and **B**) in the formation of **2** and **3**, and to characterize the bonding and electronic structure of the elusive nitrogen-centered radical in **A**.

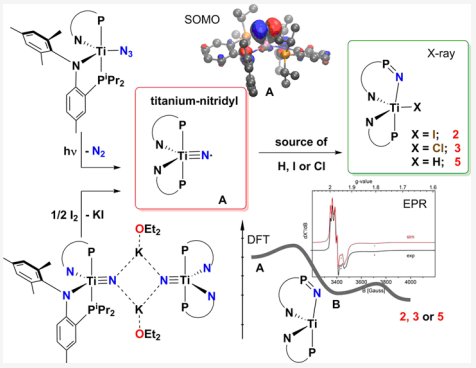

INTRODUCTION

Unlike the ubiquitous oxygen-centered radicals that play vital roles in life-sustaining processes such as respiration,[1] formation of biological reagents, and biodegradation of toxic compounds in the body (cytochromes),[2,3] nitrogen-centered radicals are just now beginning to enter the stage.[4] These less-studied radicals are also vital, given their roles in dinitrogen splitting (and its microscopic reverse step, N−N bond formation),[5−25] radical-ejection or atom-abstraction processes,[26−33] as well as C−H insertion reactivities.[34−42] More recently, the role of nitrogen-centered radicals in catalytic reactions involving aminyl (radical on a -NR_2 or -NHR) or imidyl (radical on a NR^{2-}) radicals is just now beginning to be exploited for the construction of amines or N-based heterocycles.[35] While amidyl and imidyl metal species contain a more secluded and delocalized radical, nitridyl species are far more scant, given the more exposed nitrogen-centered radical. As a result, nitridyls have a propensity to undergo reductive coupling, bridging, or oligomerization, to delocalize the unpaired electron or undergo atom-abstraction reactions. To date, there are only a few examples of (meta)stable mononuclear nitridyl complexes that have been detected spectroscopically, namely, the radical cation $[(PNP)Ir(N\bullet)][PF_6]$ or its neutral derivative (PNP)-Ir(N•) (PNP^- = $[\{(^tBu_2P)(CHCH)\}_2N]$), which are stable at room temperature for several minutes (Scheme 1).[43] Another example of a stable nitridyl species is the bridging dirhodium complex $[(PNN)Rh]_2(\mu_2\text{-}N)$ (PNN = 6-di(*tert*-butyl)-phosphinomethyl-2,2′-bipyridine) shown in Scheme 1, which allows the unpaired electron to delocalize across the topologically linear Rh=N=Rh linkage.[44] However, other likely nitridyl candidates that merit mention based on computational predictions are tetragonal Fe(IV) species of the type $[(cyclam)Fe(N)]^{2+}$ (cyclam = 1,4,8,11-tetrazacyclotetradecane) which are stable under frozen matrix condition[45,46] or the tetranuclear Fe nitride complex $[K]_2[Fe_4N_2(nacnac)_4Cl_2]$ ($nacnac'^-$ = $[ArNC(CH_3)]_2C(CH_3)$, Ar = 2,6-$Me_2C_6H_3$) derived from reductive N_2 splitting, the latter of which also provides a medium to delocalize the radical on nitrogen.[47]

In 2012, we referred to the term nitridyl for the first time, via the likely intermediate (nacnac)Ti(≡N•)($Ntol_2$) ($nacnac^-$ = $[ArNC(CH_3)]_2CH$, Ar = 2,6-$^iPr_2C_6H_3$, tol = 4-$CH_3C_6H_4$)[29]

Received: December 13, 2020
Published: April 7, 2021

https://doi.org/10.1021/acs.inorgchem.0c03644
Inorg. Chem. 2021, 60, 5635−5646

Scheme 1. Examples of Spectroscopically Characterized Iridium Nitridyl Complexes (2012), and the Spectroscopically and Structurally Characterized Dirhodium Nitridyl (2014) by the de Bruin and Schneider Groups

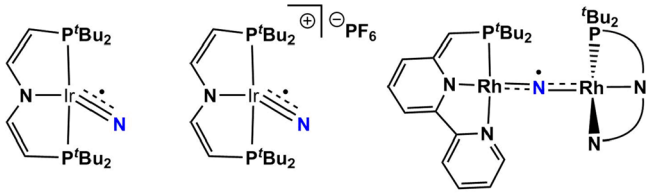

formed en route to the parent imido (nacnac)Ti(≡NH)-($NHtol_2$), the latter being isolated and fully characterized. Although transition metal nitridyl species are generally produced via N_2 extrusion from an azide precursor $L_nM^n(N_3)$ to afford the two-electron metal oxidized radical species $L_nM^{n+2}(N)$,[48] our approach using early transition metals takes advantage of the fact that the radical being generated is intuitively expected to be fully nitrogen-centered (with very little, if any, delocalization into π-bonds or metal *d* orbitals). Such a goal can be accomplished since the metal ion bearing the azido ligand can only be oxidized by one-electron, namely $L_nM^{n+1}(N\bullet)$, given that it has already reached its highest formal oxidation state. As a result, this transient moiety is expected to be quite reactive, thus resulting in immediate radical reactions such as H atom abstraction to produce the parent imide $L_nM^{n+1}(NH)$.[29−31]

Recently, we reported the synthesis and substitution reactions of a terminal molecular titanium nitride anion $[(PN)_2Ti{\equiv}N(\mu_2\text{-}K(OEt_2)]_2$,[49,50] supported by two PN ligands, (PN^- = (*N*-(2-P^{i}Pr$_2$-4-methylphenyl)-2,4,6-$Me_3C_6H_2$). Since two PN ligands chelate to the metal center, the system can be interchanged with minimal energy between geometries, such as trigonal bipyramidal and square pyramidal, while taking advantage of the pseudo tetragonal geometry ideal for metal−nitrogen multiple bonding with the nitride. Given the powerful nucleophilicity of the nitrido moiety[49,50] and its ability to make metal−ligand multiple bonds, we inquired if it would be possible to oxidize the nitride anion to independently generate a titanium nitridyl of the type $(PN)_2Ti(\equiv N\bullet)$ (**A**). Our study described here is aimed at understanding how the elusive transient titanium nitridyl, **A**, is likely produced by two independent reactions and how these processes lead to divergent reactivity−dinitrogen extrusion from the Ti(III)

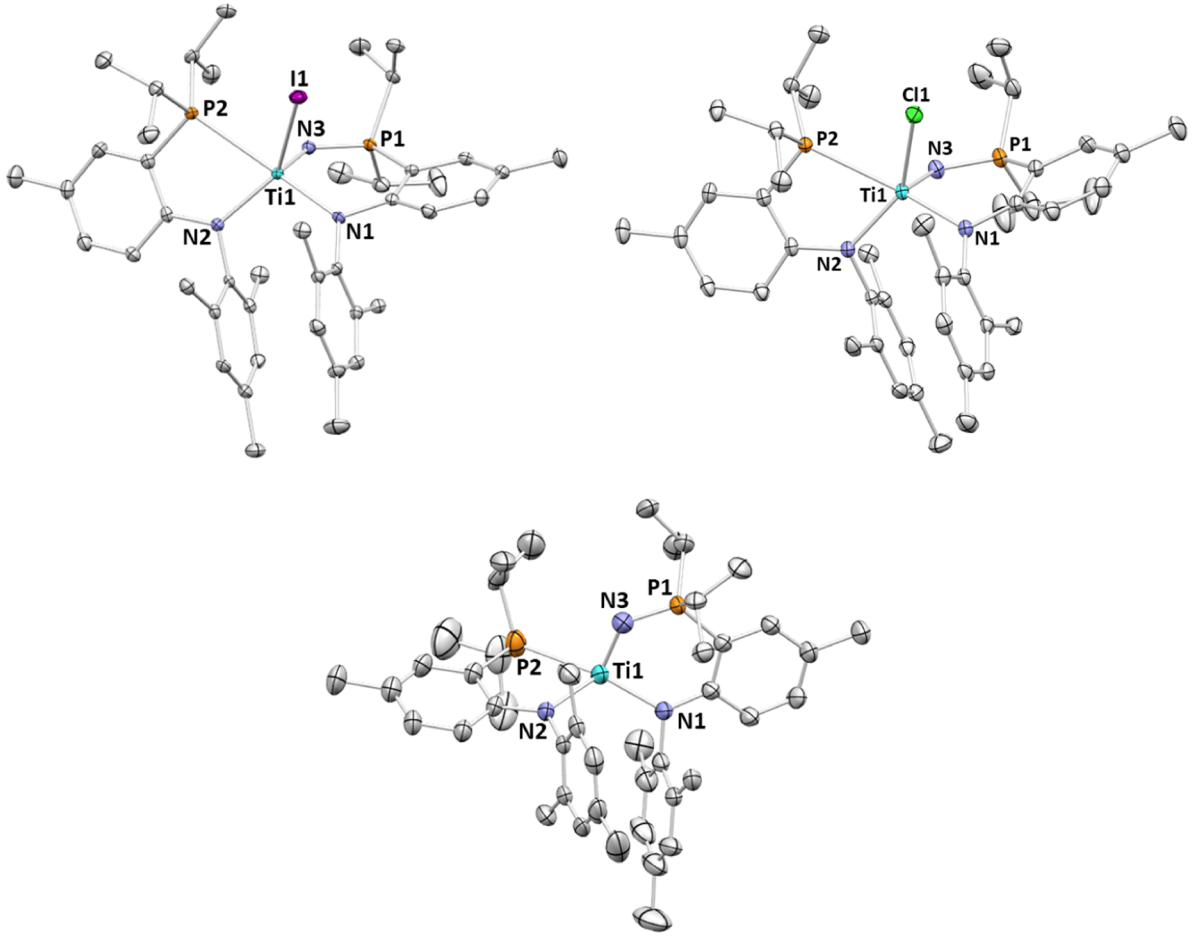

Figure 1. Solid-state structures of complexes **2** (top left), **3** (top right), and **5**, (lower) displaying thermal ellipsoids at the 50% probability level. H atoms, a molecule of *n*-hexane in **2**, half molecule of residual dimethoxyethane in **3**, and two molecules of **5** have been omitted for clarity. Only one of the crystallographically independent molecules of **2** has been pictured. Selected distances (Å) for **2**: Ti1−N1, 2.009(2); Ti1−N2, 2.041(2); Ti1−N3, 1.786(2); Ti1−P2, 2.6616(8); Ti1−I1, 2.7920(5); for **3**: Ti1−N1, 2.0329(18); Ti1−N2, 2.0436(18); Ti1−N3, 1.7867(18); Ti1−P2 2.6514(7); Ti1−Cl1, 2.3801(6); for **5**: Ti1−N1, 2.005(3); Ti1−N2, 2.045(4); Ti1−N3, 1.761(4); Ti1−P2 2.644(2).

https://doi.org/10.1021/acs.inorgchem.0c03644
Inorg. Chem. 2021, 60, 5635−5646

azide precursor, $(PN)_2Ti(N_3)$, and one-electron oxidation of a titanium nitride anion $[(PN)_2Ti{\equiv}N]^-$ using weak inner-sphere oxidants such as I_2 and $ClCPh_3$. The following work describes how a nucleophilic nitride of an early transition metal can be converted to a radical intermediate (or alternatively called electrophilic nitride) by virtue of a one-electron oxidation reaction. In this study, we showcase a combination of spectroscopic analyses and chemical oxidations studies as suitable entryways to elucidate the nature of the transient early transition metal nitridyl fragment in putative **A**.

RESULTS AND DISCUSSION

A Likely Titanium Nitridyl Generated from One-Electron Oxidation of a Titanium Nitride Anion. When the previously reported titanium nitride complex, $[(PN)_2Ti{\equiv}N\{\mu_2\text{-}K(OEt_2)\}]_2$ (**1**)[49] was treated with a toluene solution containing two equiv of I_2, an immediate color change from orange to deep red was observed. The reaction mixture was stirred at room temperature for an additional 12 h, and after workup and crystallization of the reaction mixture, a ^{31}P NMR spectrum of a sample revealed the presence of two inequivalent resonances at 14.6 ppm along with a more downfield resonance at 34.9 ppm, implying that the original C_{2v} symmetry in the nitride dimer, **1**, was no longer retained. Examination of the mixture also revealed the reaction to be incomplete given the presence of **1**. Interestingly, vacuum transfer of the volatiles from the reaction mixture showed the formation of H_2 (^1H NMR: 4.47 ppm) in addition to free Et_2O (stemming from complex **1**). Notably, the gas produced in the reaction was irrefutably shown to be H_2 by an additional control experiment involving the hydrogenation of styrene to ethylbenzene in presence Pd/charcoal (Figure S16).[51] To elucidate the connectivity of this new complex, a single crystal X-ray diffraction study was performed on an isolated single crystal, obtained from a concentrated *n*-hexane solution stored at −35 °C. (Figure 1, top left). Inspection of the solid-state structure shows that the former nitride was inserted into one of the phosphorus arm of the PN^- ligand, making this scaffold into an asymmetrical NPN' unit which contains a phosphinimide fragment, namely, one of the ligands in compound (NPN')(PN)Ti(I) (**2**) (NPN'^{2-} = N-(2-NP^iPr_2-4-methyl-phenyl)-2,4,6-$Me_3C_6H_2$). Complex **2** can be isolated in 48% yield from the reaction mixture (Scheme 2), and it was found that the same species could be alternatively prepared from **1** and ICH_2CH_2I (see SI). These solid-state structural features are retained in solution and corroborate the two inequivalent and downshifted phosphorus environments observed in the ^{31}P NMR spectrum at δ 34.9 and 14.6 ppm (Figure S2); one resonance for the unaltered PN^- ligand along with the more downfield resonance attributable to the phosphinimide arm of the ligand NPN'^{2-}.

While our previously reported 5-coordinate complexes with two PN^- ligands have been closer to trigonal bipyramidal in geometry with τ_5[52] values ∼0.7−0.8, **2** has a value instead confined between the two geometries (τ_5 = 0.52) for one of the two crystallographically inequivalent (but chemically equivalent) molecules within the asymmetric unit with N1−Ti1−P2 = 168.25(7)° and N2−Ti1−I1 = 137.08(6)°. Interestingly, the second independent molecule has a more distorted τ_5 = 0.35 due to the differing angles of N1'−Ti1'−P2' = 162.52(7)° and N2'−Ti1'−I1' = 141.78(7)°, indicating that both molecules are quite distorted, but on average, complex **2** favors a square pyramidal geometry.

Scheme 2. Reaction of 1 with the Weak and Inner-Sphere Oxidants I_2 and $ClCPh_3$ to Yield the Phosphinimide Complexes 2 and 3, Respectively

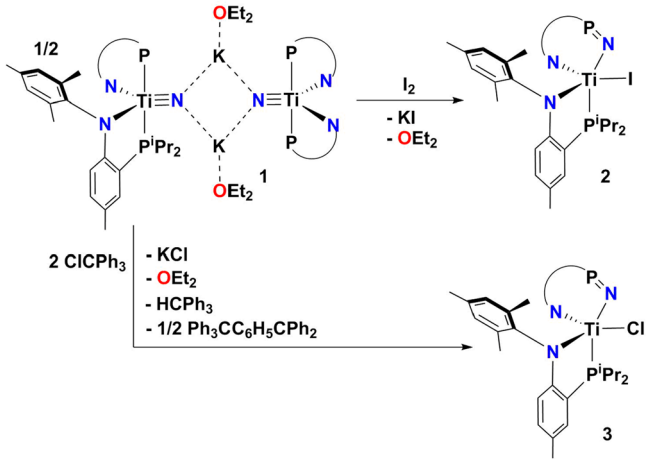

Since I_2 can be a troublesome oxidant to handle (e.g., volatile, two-electron oxidant), we resorted to the use of a different oxidant that could allow us to observe the formation of a radical. When complex **1** was treated with two equiv of $ClCPh_3$, an oxidant with a similar oxidation potential to I_2 (−0.11 vs −0.14 V, respectively vs SCE), an immediate color change from orange to dark red was also observed. However, since this is a one-electron oxidant unlike I_2, it was confirmed that four equiv of $ClCPh_3$ were needed in order to achieve full consumption of the starting material, **1**. After workup and crystallization of the mixture from hexane at −35 °C, the chloride analogue of **2**, (NPN')(PN)TiCl (**3**) was isolated in 49% yield (Scheme 2) based on its spectroscopic similarity to **2** (^{31}P NMR spectrum showed two singlet resonances at δ 12.1 and 35.1 ppm, Figure S6, Supporting Information) as well as connectivity confirmed by single crystal X-ray diffraction studies. Interestingly, and unlike the I_2 oxidation, examination of the reaction mixture by ^1H NMR spectroscopy revealed the formation of $HCPh_3$ and Gomberg's dimer, $Ph_3CC_6H_5CPh_2$ (Scheme 2). As shown in Figure 1, complex **3** instead favors an even more square pyramidal geometry (τ_5 = 0.16),[52] likely due to less steric hindrance in the axial position of a chloride vs the iodide (N2−Ti1−P1 = 153.68(6)° and N1−Ti1−Cl1 = 144.21(6)°). The insertion of the formal nitrido ligand into the phosphine group of the PN ligand tantalizingly suggests that a transient nitridyl moiety is generated upon oxidation of **1**. The oxidation of a phosphine by a nitride ligand is consistent with this moiety being electrophilic in nature, akin to those observed in Fe(IV) nitrides.[53−58] However, we were puzzled by the accompanied formation of molecular H_2 with **2** as well as $HCPh_3$ with **3**.

To establish the source of the hydrogen atom (proton or hydride) that resulted in formation of H_2 or $HCPh_3$, the parent imido complex, $(PN)_2Ti{\equiv}NH$ (**4**) was examined, since this species could provide mechanistic insight. Previously, we reported that a rare example of a parent imido complex **4** could be prepared via treatment of **1** with $HN\{SiMe_3\}_2$ (HMDS).[50] It was found that phenol was a more convenient proton source to afford **4** in greater yields, given the insolubility of KOPh as opposed to $KN\{SiMe_3\}_2$ (Scheme 3). Surprisingly, it was found that complex **4** would gradually transform to a new previously unidentifiable major species proposed to be

https://doi.org/10.1021/acs.inorgchem.0c03644
Inorg. Chem. 2021, 60, 5635−5646

Scheme 3. Synthesis of a Mixture of Parent Imido, 4 and the N-Inserted Hydride, 5 from the Photolysis of the Ti(III) Azide Precursor, 6

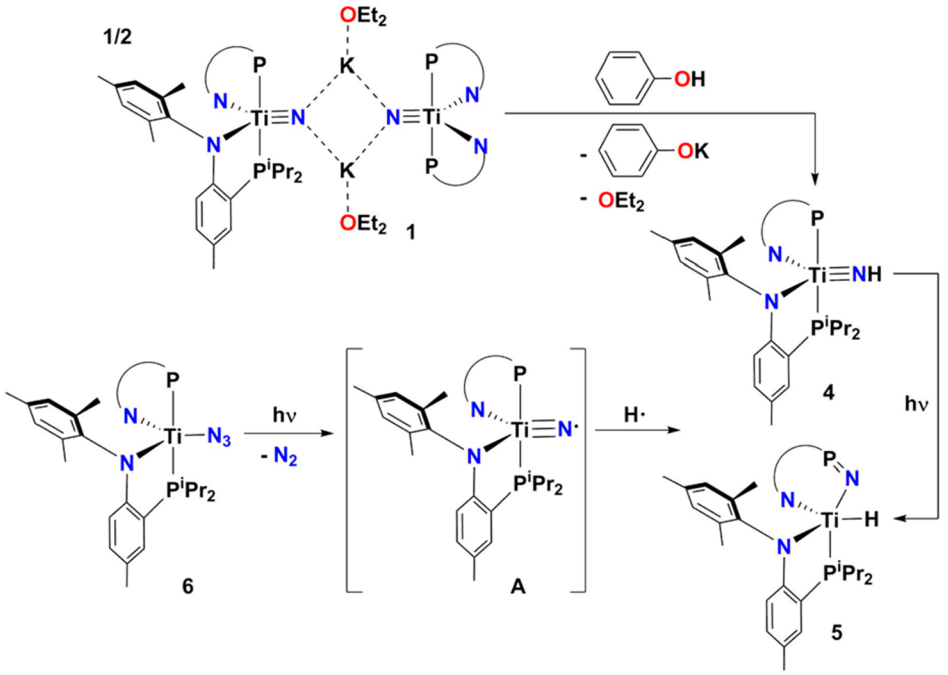

(NPN')(PN)Ti(H) (**5**) (Scheme 3). Akin to **2** and **3**, the ^{31}P NMR spectrum of this new material indicated the presence of two chemically inequivalent phosphorus ligand environments at δ 7.4 and 22.3 ppm (Figure S13). After several control reactions, it was established that **4** sluggishly converts to **5** in benzene under photochemical conditions (several days in room light).

This conversion is arrested if the sample is isolated and stored in the dark. To determine if the new species could indeed be an insertion product such as a titanium hydride, **5**, based on similar reactivity observed in the oxidation reactions shown in Scheme 2 (*vide supra*), pure samples of **4** were subjected to photolysis using a xenon lamp source. Accordingly, the ^{31}P NMR spectrum of this mixture showed complete conversion of **4** to **5** after 15 min of irradiation (Figure S13). In solution, complex **5** shows all the features expected for a Ti(IV) complex based on ^{31}P and ^{1}H NMR spectral data, although there are no salient resonance features in the ^{1}H NMR spectrum to assign this complex since it was not possible to spectroscopically observe the hydride resonance. Only the ^{31}P NMR spectrum provided clear evidence for complex **5** possessing two distinctly inequivalent resonances at δ 7.4 and 22.3 ppm, where the latter is attributable to the phosphinimide resonance, similar to the observed spectral data of **2** and **3**, *vide supra*.

Crystallization of the highly lipophilic complex from a saturated pentane solution at −35 °C overnight resulted in the deposition of few dark red single crystals of the tentative N-inserted product, **5**. Due to poorly diffracting crystals, even when crystallized from a variety of different solvents, it was not possible to locate the hydride ligand in the difference map (bottom, Figure 1). However, the solid state of **5** does reveal overall gross connectivity showing both the phosphinimide and unharmed PN ligand in [(NPN')(PN)Ti].

Attempts were made via a deuterium labeling study to unequivocally and spectroscopically assign the hydride ligand in complex **5**. Accordingly, complex **1** was treated with phenol-d_6, immediately forming the parent deuteride complex (PN)$_2$Ti≡ND (**4**-d_1), and the ^{2}H NMR spectrum of this isotopologue shows the anticipated N−*D* resonance at 5.0 ppm (Figure S11); a spectroscopic feature observed in the ^{1}H NMR spectrum for unlabeled **4**. Likewise, the ^{31}P NMR spectrum of **4**-d_1 shows the similar resonance observed in **4** at δ 15.5 ppm (Figure S12). In addition, the IR spectrum of **4** shows an N−H stretch at 3398.9 cm^{-1}, which greatly shifts as expected to 2517.6 cm^{-1} for N−D stretch in deuterated **4**-d_1 (Figures S17, S18). Having characterized the isotopologue **4**-d_1, we then photolyzed it to (NPN')(PN)Ti(D) (**5**-d_1) and monitored the reaction by ^{31}P NMR spectroscopy via its comparison to unlabeled **5**. Despite multiple attempts, however, ^{2}H NMR spectral data of **5**-d_1 was still ambiguous and did not clearly reveal the characteristic Ti−D (or Ti−H) resonance at lower fields,[59−63] akin to those reported for a few examples of titanium hydrides. However, it cannot be ruled out that such a hydride resonance might be broadened due to both ^{31}P and ^{14}N coupling. Unfortunately, there are also no distinct features in the IR spectrum for both the hydride and the deuteride isotopologue of **5**. Gratifyingly, however, we were able to show the presence of a hydrido ligand in **5** by addition of a stoichiometric quantity of ClCPh$_3$ to a solution of **5** in C$_6$D$_6$. Examination of this reaction mixture by ^{1}H NMR spectroscopy demonstrated the quantitative formation of **3** along with HCPh$_3$, thus providing experimental evidence for the former hydride moiety being present in **5**.

In Pursuit of a Transient Titanium Nitridyl by Incomplete Azide Reduction. Intrigued by the insertion of the nitridyl nitrogen of a likely species such as **A** into the phosphorus arm of the ligand, we inquired if this reactive motif could be accessed via other routes to better understand their mode of reactivity and mechanism of formation. The nitrogen atoms in the ubiquitous azide ligand, N_3^-, carry each a formal oxidation state of −1/3. Upon reduction by two electrons, the

https://doi.org/10.1021/acs.inorgchem.0c03644
Inorg. Chem. 2021, 60, 5635−5646

Scheme 4. Proposed Pathways (Path A and Path B) Involving the Oxidation of Nitride 1 to the Phosphinimide Complexes 2 and 3, with I_2 and $ClCPh_3$, Respectively

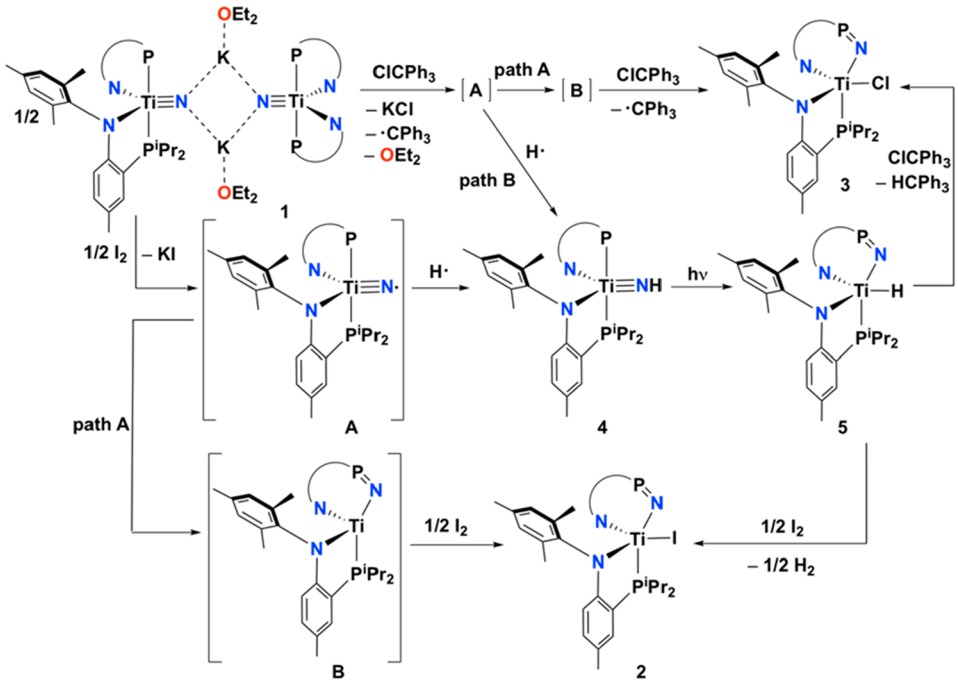

azide ligand fragments to N_2 and N^{3-}, the latter which carries a formal oxidation state of −III (eq 1a). However, if one reduces an azide by one-electron while promoting N_2 extrusion, one could, in principle, produce a nitridyl nitrogen instead a formal oxidation state of −II (eq 1b). Previously, our group reported the synthesis of a stable Ti(III) azide complex, $(PN)_2Ti(N_3)$ (**6**),[49] which upon reduction by one electron with KC_8 produced the nitride complex **1**, *vide supra*, in accordance with the simplified reaction shown in eq 1a. In such a transformation, the Ti(III) supplied one electron while the KC_8 provided the second one needed to effect N_3^- fragmentation to the satisfied valencies on nitrogen. However, when a sample of **6** (in the absence of exogenous reductant) was dissolved in deuterated benzene as a dilute solution (10−15 mM) and was irradiated with a xenon lamp source for a period of 5 min in an NMR tube fitted with a J-Young valve, the ^{31}P and ^{1}H NMR spectral data of the reaction mixture allowed for identification of the parent imido and insertion complexes, respectively, **4** and **5**, along with other side-products we have been unable to identify (Scheme 3). Despite this, complete conversion of **4** to **5** can be achieved if the mixture is photolyzed for an additional 10 min, in accordance with what we previously observed for independently prepared samples of pure **4** photolyzed for the same period of time (Scheme 3).

$$N_3^- + 2e^- \rightarrow N_2 + N^{3-}(\text{nitride}) \quad (1a)$$

$$N_3^- + 1e^- \rightarrow N_2 + N^{\bullet 2-}(\text{nitridyl}) \quad (1b)$$

Reactivity Studies to Understand Formation of 2 and 3 From Nitride 1 and Oxidants I_2 and $ClCPh_3$. Insertion of the formal nitrido nitrogen into the phosphine arm of one of the PN^- ligands suggests that an electron deficient nitride is likely formed in the course of these reactions. Since I_2 and $ClCPh_3$ can serve as weak and inner-sphere oxidants and radical traps, the reactions were monitored in order to observe intermediates or side products, likely deriving from what we propose to be the putative transient nitridyl, **A**. Accordingly, treatment of **1** with I_2 resulted in the immediate formation of **2** and **4**, along with the hydride **5**, the latter which, over time, was observed to convert to **2**. It was determined that the reaction required approximately two equiv of I_2 per equiv of **1** in order to proceed to completion. As noted before, examination of volatiles unambiguously revealed formation of molecular hydrogen as one of the side products from this reaction (Figure S4, Supporting Information). It was also found that conducting the reaction in the dark also led to formation of less than 50% of **2**, with the remainder of the mixture being attributable to **4**. Under these conditions, only traces of **5** were spectroscopically detected by ^{31}P NMR spectroscopy, suggesting that **5** most likely derives from the photochemical conversion of **4**. Indeed, control experiments using independently prepared **4** reveal that reaction with I_2 produces H_2 and **2** when exposed to light, and that such gas is indeed H_2 since it hydrogenates styrene (*vide supra*).[51] Interestingly, when complex **1** is oxidized instead with ICH_2CH_2I, no H_2 is observed (only ethylene), with the only titanium product produced being **2**. If instead, the control experiment having a mixture of **4** with H_2 is left in the absence of light, no reaction proceeds. On the basis of this premise, the hypothesis is that the formation of **2** from I_2 oxidation of **1** occurs via two plausible routes labeled as path A and path B (Scheme 4). In the first step, one-electron oxidation of each nitride ligand in **1** with one equiv of I_2 results in formation of KI and likely a transient nitridyl **A**, which can either abstract H atom to form the parent imide **4** (path B) or undergo insertion into the phosphine arm to produce the phosphinimide Ti(III) radical (NPN')(PN)Ti (**B**) (path A). In the presence of additional I_2, species **B** would rapidly become oxidized to **2**. Meanwhile, photochemical conversion of complex **4** to **5** would allow any unreacted I_2 to oxidize the hydride by producing **2** and 1/2 equiv of H_2. As stated previously, we

https://doi.org/10.1021/acs.inorgchem.0c03644
Inorg. Chem. 2021, 60, 5635−5646

shifted our attention to the one-electron oxidant and hydride abstractor $ClCPh_3$, which, in addition to the benefits described above, is also a stable solid that can be easily weighed and scaled to experiments for NMR spectroscopic measurements. As stated before, we predicted that $ClCPh_3$ would qualitatively react with the hydride in **5** and lead to formation of $HCPh_3$. Likewise, $ClCPh_3$ can also allow for identification of its radical, via formation of Gomberg's dimer.[64] Accordingly, treatment of one equiv of **1** with four equiv of $ClCPh_3$ in C_6D_6 in the presence of light over 15 min resulted in the formation of one equiv of Gomberg's dimer, along with two equiv of **3** and $HCPh_3$, both of which were detected by a combination of ^1H and ^{31}P NMR spectroscopic experiments. In these NMR experiments, **4** is not observed, unless the reaction is maintained in the dark, in which the imide does not transform to the reactive hydride species. Conduction of the same experiment in the absence of light resulted also in formation of Gomberg's dimer, **3**, and the imide **4**, therefore suggesting that $HCPh_3$ derives from hydride abstraction of **5** with $ClCPh_3$. This result unequivocally demonstrates the presence of a hydride ligand in **5** despite the lack of spectroscopic and unambiguous structural evidence. Indeed, addition of $ClCPh_3$ to a benzene-d_6 solution of independently prepared **4** in the presence of light cleanly results in formation of **3** and $HCPh_3$. As a result, our proposed pathway in Scheme 4 shows how paths A and B both result in formation of **2** and **3** by the addition of oxidants I_2 or $ClCPh_3$, respectively, to nitride **1**. Paths A and B both could share the formation of common transient nitridyl intermediate **A**, which can either oxidize a proximal phosphine P of the PN^- ligand (path A) or abstract an H atom (path B). As will be demonstrated, frozen matrix conditions can allow us to avoid the H atom abstraction pathway and spectroscopically identify the formation of a species such as **B**.

Attempts to Spectroscopically Observe the Radical Intermediates A and B. It was predicted that intermediate **A** would be expected to be reactive and nonisolable under normal reaction conditions. As a result, frozen matrix X-band EPR studies of **6** were performed under photolytic conditions. The azide precursor complex **6** reveals a rhombic EPR spectrum with partially resolved hyperfine interactions (HFIs) with two inequivalent P-nuclei. A satisfactory simulation of the experimental X-band EPR spectrum (Figure 2) was obtained with the following parameters: g_{11} = 1.9725, g_{22} = 1.9330, g_{33} = 1.8030; $A^{P1}{}_{11}$ = 65 MHz, $A^{P1}{}_{22}$ = 75 MHz ($A^{P1}{}_{33}$ not resolved); $A^{P2}{}_{11}$ = 45 MHz, $A^{P2}{}_{22}$ = 55 MHz ($A^{P2}{}_{33}$ not resolved).

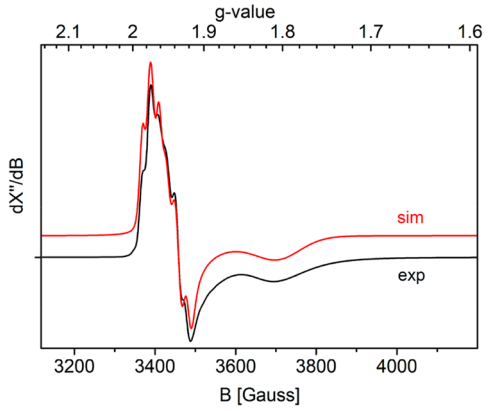

Figure 2. Experimental and simulated EPR spectrum of **6**. Experimental parameters: temperature 20 K, solvent: toluene, microwave frequency = 9.363322 GHz, microwave power = 0.632 mW, mod. ampl. = 4 G.

Unfortunately, the EPR spectrum obtained directly after photolysis of azide complex, **6**, at 20 K using a strong UV lamp (270−600 nm range, glass fiber technology), was not entirely clean and gave rise to somewhat broadened spectra. However, warm-up of the sample after photolysis followed by rapid refreezing of the sample led to the fairly clean spectrum shown in Figure 3 (top). The thus obtained X-band EPR spectrum

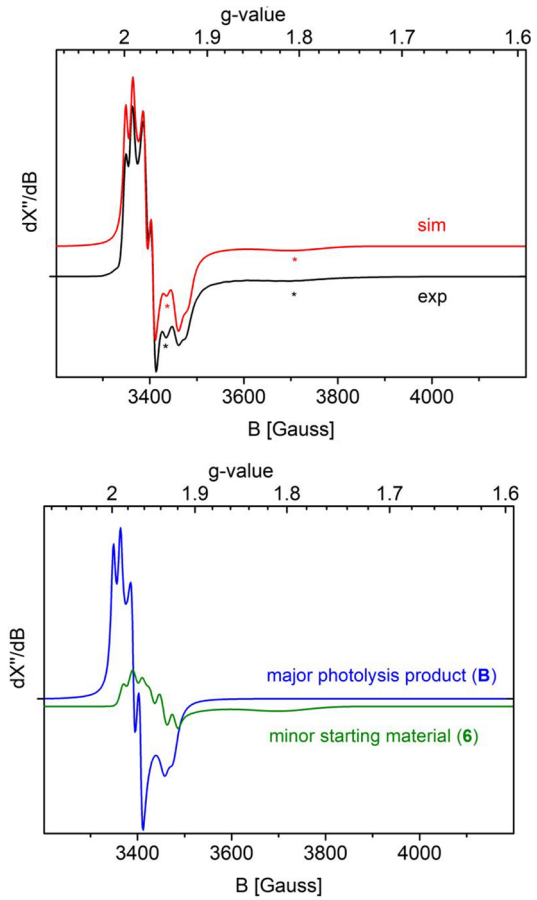

Figure 3. *Top:* Overlay of the experimental (black) and simulated (red) EPR spectra of species **B** obtained after photolysis of **6** (signals marked with * stem from some remaining azide starting material **6**). Experimental parameters: Temperature 20 K, solvent toluene, microwave frequency = 9.362333 GHz, microwave power = 0.632 mW, mod. ampl. = 4 G. Parameters used in in the simulation are shown in Table 1. *Bottom:* Separated spectra of the species contributing to the simulated spectrum: Major photolysis product **B** (blue) and minor starting material **6** (green).

contains some remaining starting material **6** (indicated with *) but reveals formation of a single photolysis product as the major compound (Figure 3, bottom; blue trace). The same signals are also detected during the photolysis experiment performed at 20 K in the EPR cavity before warming-up the sample. The signals of the photolysis product stem from a Ti(III) species with a rhombic *g*-tensor (g_{11} = 1.9930; g_{22} = 1.9680; g_{33} = 1.9295) and resolved HFIs with one P-nucleus in all directions ($A^{P1}{}_{11}$ = 42 MHz, $A^{P1}{}_{22}$ = 45 MHz; $A^{P1}{}_{33}$ = 50 MHz). Notably, it is clear that the signals of the photolysis product reveal HFIs with a *single* P-nucleus, while those of the

https://doi.org/10.1021/acs.inorgchem.0c03644
Inorg. Chem. 2021, 60, 5635−5646

starting material **6** reveal clear HFIs with *two* (inequivalent) P-nuclei (*vide supra*). Furthermore, it is worth mentioning that the measured *g*-values and HFIs are *not* in agreement with the DFT calculated values of transient nitridyl complex **A** (Scheme 5 and Table 1). The experimental data are, however, in reasonable agreement with the DFT computed g-values and phosphorus HFIs of radical insertion product **B** (Schemes 4 and 5; Table 1). Hence, the obtained EPR spectral data suggest that photolysis of **6**, under conditions (at 20 K) where hydrogen atom transfer (HAT) is prevented, leads to rapid formation of species **B**, presumably via facile nitrogen insertion into the proximal Ti−P bond of the apparently unstable species **A** (Scheme 5).[65]

Scheme 5. Frozen Matrix Photolysis of Azido Species 6 at 20 K, Forming Nitridyl Species A, after Which the N Atom Inserts into the Proximal Ti−P Bond, in an Apparently Low Barrier Transformation

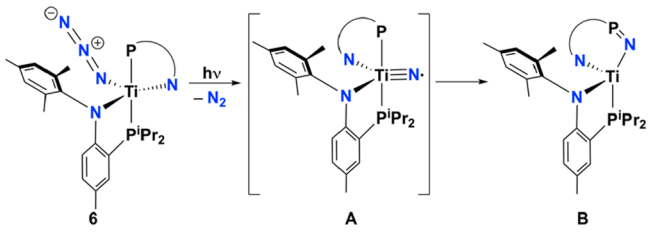

Table 1. Experimental EPR Parameters[a] of the Species Formed after Photolysis of Species 6 at 20 K, Compared with the DFT Calculated Values[b] of Nitridyl Species A and Insertion Product B

	Exp.	species A (DFT)	species B (DFT)
g-values			
g_{11}	**1.993**	**2.012**	**1.998**
g_{22}	**1.968**	**2.005**	**1.965**
g_{33}	**1.930**	**2.002**	**1.929**
Hyperfine interactions (MHz)			
$A^{P1}{}_{11}$	**42**	**5.6**	**−42.1**
$A^{P1}{}_{22}$	**45**	**6.1**	**−30.0**
$A^{P1}{}_{33}$	**50**	**10.3**	**−15.9**
$A^{P2}{}_{11}$	**NR**	**7.4**	**−0.3**
$A^{P2}{}_{22}$	**NR**	**8.3**	**1.9**
$A^{P2}{}_{33}$	**NR**	**14.1**	**2.7**
$A^{N1}{}_{11}$	NR	−1.0	−6.2
$A^{N1}{}_{22}$	NR	−1.0	−4.8
$A^{N1}{}_{33}$	NR	22.7	−4.7
$A^{N1}{}_{11}$	NR	−1.7	−7.4
$A^{N1}{}_{22}$	NR	−1.3	−5.2
$A^{N1}{}_{33}$	NR	25.5	−4.7
$A^{N3}{}_{11}$ (*"nitride"*)	NR	−13.2	−8.1
$A^{N3}{}_{22}$ (*"nitride"*)	NR	−11.3	−5.7
$A^{N3}{}_{33}$ (*"nitride"*)	NR	36.4	−4.2

[a]Parameters extracted from the experimental spectrum using spectral simulation. NR = not resolved. [b]ADF, BP86, TZP.

The fact that we were unable to detect nitridyl species **A** with EPR spectroscopy during photolysis of **6** suggests that even under these matrix frozen conditions, N atom insertion into one of the Ti−P bonds of species **A** (pathway B) is rapid (Scheme 4). Spectroscopic data under these conditions reveal no sign of transient **A** being present, which is perhaps not too surprising since formation of the nitridyl is most likely rate-determining and the **A** must be a high energy species. It is therefore quite possible that under the latter conditions, an intramolecular N atom rearrangement pathway becomes preferred over HAT. This could be more prominent in solution, and HAT may involve a thermal pathway as opposed to a photochemical one. To address the source of the H atom resulting in formation of **4**, several control and isotopically labeled experiments were conducted. It was found that conducting of photolytic reactions of **6** in deuterated solvent (toluene-d_8 or benzene-d_6) did not result in any detectable amount of the isotopomer **4**-d_1 when assayed via ^{2}H NMR spectroscopy, therefore ruling out solvent as the source of hydrogen. Likewise, NMR spectroscopic samples of photolyzed **6** using an internal standard of triphenylphosphine resulted in the quantification of **4** in 48% yield, thus providing a compelling argument that the source of the H atom in question was indeed from ligand cannibalization. Furthermore, experiments with H atom sources such as 1,4-dihydroanthracene or 1,3-cyclohexadiene (in large excess) showed no improvement in the yield, whereas, conducting of the same reaction in concentrated or dilute conditions also did not improve the yield of **4**. Lastly, no evidence for formation of diphenyl or dibenzyl stemming from homocoupling reactions was found when such reactions were conducted in either benzene or toluene, respectively. As a result, we propose that the source of the H atom in **4** stems from the more vulnerable benzylic groups of the PN ligand scaffold in an intramolecular fashion, most likely followed by a second intermolecular HAT, or vice versa in accordance with Scheme 6. To further understand the source of the H atom and the fate of the ligand degradation leading to **4**, a reaction mixture of the products resulting from the photolysis of **6** was quenched with methanol-d_4. However, NMR spectroscopic studies of the reaction mixture showed no resonances attributable to the HPN ligand or any of its isotopomers. Likewise, it has not been

Scheme 6. Proposed Intermediates Stemming from an Intramolecular HAT Abstraction in A, Followed by a Second HAT Step Resulting in Formation of 4 and Most Likely a Decomposed Titanium Side Product

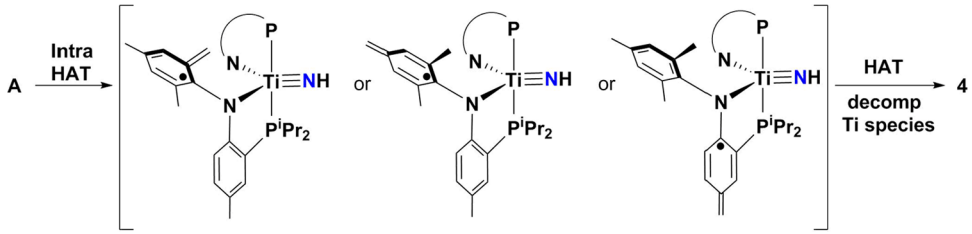

https://doi.org/10.1021/acs.inorgchem.0c03644
Inorg. Chem. 2021, 60, 5635−5646

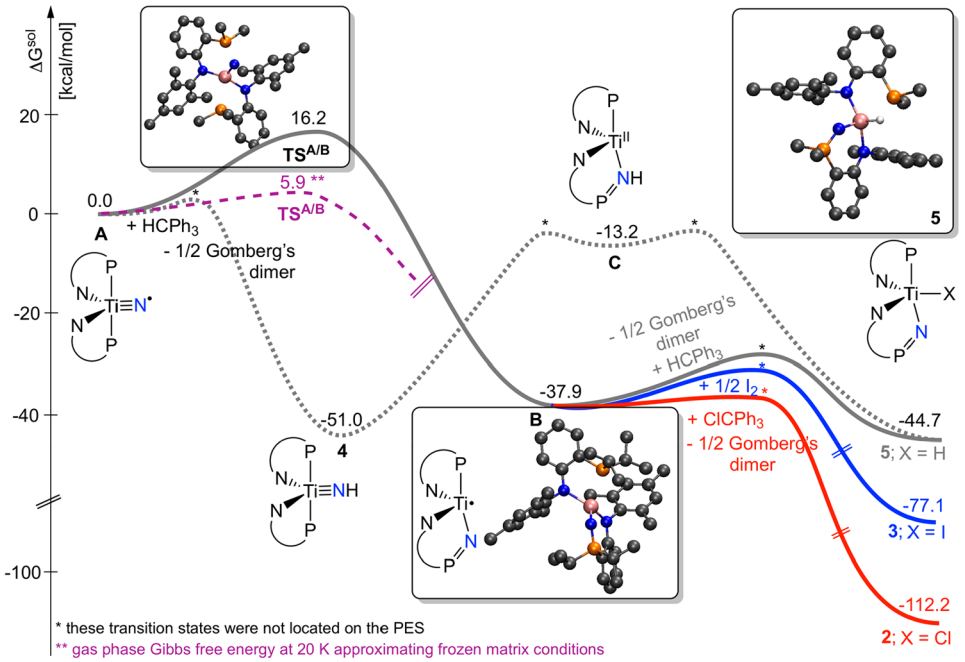

Figure 4. Solution-state Gibbs free energy profile of nitridyl (**A**) insertion into the Ti−P bond to form phosphinimide Ti(III) intermediate (the gas phase relative Gibbs free energy of $TS^{A/B}$ at 20 K is also given as an approximation for the frozen matrix condition applied in some of our experiments), **B**, and subsequent formation of hydride (**5**), iodide (**3**), and chloride (**2**) through the reaction with $HCPh_3$ (gray), I_2 (blue), and $HCPh_3$ (red). The dashed gray curve portrays the energy profile for the nitridyl **A** + $HCPh_3$ → imide **4** + 1/2 Gomberg's dimer transition together with the relative stability of intermediate **C** in the singlet state (see text) en route to the hydride **5**. The instability of intermediate **C** to **4** (37.8 kcal mol^{-1}) intuitively accounts for the lack of hydride formation from **4** in a thermal process.

possible to isolate and characterize other side-products formed after isolation of **4** from the reaction mixture involving the photolysis of **6**. Although it is not possible to directly detect *in situ* generated intermediate **A** through EPR spectroscopic studies, it is logical to propose that these results should not have the same outcome as those of the solution phase studies conducted at much higher temperatures. However, these studies lend some support to our proposed mechanism shown in Scheme 4.

Computational Studies Scrutinizing the Titanium Nitridyl Moiety and Reaction Mechanisms. To shed light on some of the details of the proposed mechanisms at a molecular level and to scrutinize the bonding, structure, and intrinsic reactivity of the elusive nitridyl **A**, we turned to quantum mechanical calculations. Using Density Functional Theory, particularly the TPSSh functional in combination with the cc-pVTZ basis set, we modeled the insertion of the nitridyl group into the Ti−P bond (path A shown in Scheme 4) and evaluated the relative thermodynamics for the formation of the iodide/chloride/hydride species **2**, **3**, and **5**, respectively (Figure 4). In addition, we assessed the energetics of path B, i.e., the **A** → **4** reaction, together with the most plausible mechanism for the parent imido to hydride isomerization, **4** → **5** (Figure 4) as well as an alternative mechanism involving the loss of N_2 from **6** without the involvement of a nitridyl **A** using TD-DFT calculations (Figure S19).[56] Our TD-DFT results suggest that formation of **A** is more likely than a concerned N_2 extrusion step via oxidation of one of the phosphine arms of the PN ligand. As Figure 4 shows, given the solution-state Gibbs free energies for the reactions of nontruncated models, the nitridyl center of **A** inserts into the Ti−P bond at the onset of path A traversing through transition state $TS^{A/B}$ with a solution state stability of 16.2 kcal mol^{-1}, forming **B** with a phosphinimide Ti=N=P functionality and a Ti(III) center. Direct coupling of either of the I, Cl, and H radicals originating from I_2 (0.5 equiv), $ClCPh_3$, and $HCPh_3$, respectively, to this titanium(III) species, which is assumed to be a barrier-less process, allows the formation of the respective iodide **3**, chloride **2**, and hydride **5** compounds. The thermodynamics of these processes were evaluated by considering the formation of Gomberg's dimer (0.5 equiv) in the reactions of $HCPh_3$ and $ClCPh_3$ with **B**, and they were found to be strongly exergonic for the formation of all halide and hydride derivatives (**2**, **3**, and **5**) .

In contrast to path A, path B begins with an initial HAT to the nitridyl center of **A** en route to the observed imide **4**. Using $HCPh_3$ as the H• source and Gomberg's dimer as side product to adjust for the energy of the hydrogen radical in this step, the nitridyl-imide transformation is highly exergonic by −51 kcal mol^{-1}. This large thermodynamic driving force is tell-tale for the highly reactive nature of the titanium-nitridyl functionality, accounting for the lack of experimental detection of the transient species **A**.

In order to gain some insights into the subsequent, puzzling imide (**4**) to hydride (**5**) process, which takes place within minutes under irradiation conditions, we calculated the stability of the intermediate with the NH group inserted into the Ti−P bond, **C** (Figure 4), which was assumed to be an inevitable intermediate in this process. Our calculations reveal that this intermediate en route to the hydride **5** is thermodynamically rather unstable in the singlet state, lying about +38 kcal mol^{-1} higher in energy with respect to imide **4**, owing, plausibly, to such species being a Ti(II). Such a high-energy intermediate, together with the antecedent/succeeding transition states that determine the corresponding activation barriers, renders the singlet imide-hydride reaction channel

https://doi.org/10.1021/acs.inorgchem.0c03644
Inorg. Chem. 2021, 60, 5635−5646

kinetically inaccessible under standard thermal conditions. The titanium(II) intermediate **C** is, however, reasonably stable in the triplet state (having two Ti-centered unpaired electrons) with a solution-state free energy of about 15 kcal mol^{-1} to the preceding imide. In addition, TD-DFT simulation of the photoexcitation of the imide **4** exposed a prominent adsorption at 399.1 nm with oscillator strength of 0.104 corresponding to singlet−singlet electronic transition, best described as a ligand-to-metal charge transfer, LMCT, where one of the π-electrons of the PN ligand is promoted to a low-lying titanium d orbital. Although locating the minimum energy crossing points for the singlet−triplet crossover along the reaction coordinate from this singlet excited state of **4** to the triplet **C** and discovering other plausible excited state mechanisms is beyond the scope of this computational analysis, the experimental observations can be intuitively interpreted in light of these findings. Namely, the imide to hydride isomerization is not operative in the dark because the process is associated with a large activation barrier in the singlet state surface. Under irradiation, in contrast, the photoexcitation of the titanium-imide **4** is followed, plausibly, by intersystem crossing to the triplet surface; this gives access to a low-energy triplet state reaction path, characterized by the stable triplet Ti(II) intermediate **C***, therefore allowing the formation of the hydride species **5**.

In the cases when the highly reactive nature of a key species prohibits its direct characterization by experimental means, e.g., the transient nitridyl complex **A**, the insights into the structure, bonding, and reactivity gained through realistic computer simulations become invaluable.[49,50] In a previous publication, large-scale computational investigations on $[(PN)_2Ti{\equiv}N]^-$, $(PN)_2Ti{\equiv}NK(18\text{-crown-}6)$, and $[(PN)_2Ti{\equiv}N\{\mu_2\text{-}K(OEt_2)\}]_2$ demonstrated the accuracy of DFT methods for modeling the structural and spectroscopic (especially NMR) properties of these complexes.

The computed equilibrium structure of **A**, given in Figure 4, reveals an overall geometry around the metal which is very similar to that of titanium-nitrides, such as in the discrete salt of **1**, namely, the anionic component of $[K(2,2,2\text{-kryptofix})][(PN)_2Ti{\equiv}N]$, confined between a trigonal bipyramid and a square pyramid with a τ_5 value of 0.55. In particular, while the P−Ti−P angle remains close to 180° (178.7°), the largest N−Ti−N angle of 155° departs notably from 120° as well as from 180°, corresponding to the idealized values of trigonal bipyramidal and square pyramidal structures, respectively. The $Ti{-}N_{nitridyl}$ distance is computed to be 1.70 Å, which is somewhat longer than the $Ti{-}N_{nitride}$ distance of 1.66 Å in $[(PN)_2Ti{\equiv}N]^-$, implying the weakening of the Ti≡N bond upon oxidation of $[(PN)_2Ti{\equiv}N]^-$ to $[(PN)_2Ti{\equiv}N]^{\bullet}$.

To characterize the nature of the Ti≡N bond of the latter species, we analyzed its molecular electronic structure using quasi-restricted orbitals (QROs), atom localized spin densities, and bond order indices. QROs provides an inherent description of open shell molecules, such as in doublet $[(PN)_2Ti{\equiv}N]^{\bullet}$, with different α and β orbital subsets through a conceptual picture like that of the restricted open-shell solution with doubly and singly occupied orbitals (i.e., spatially identical α and β orbitals). Recently, for example, we utilized this technique to rationalize the EPR response and unique perpendicular V−PCO binding mode of a triplet V(III) complex.[66] The general molecular orbital picture of the Ti≡N bond of transient **A** is virtually the same as that of the titanium-nitride species formally comprising a Ti−N σ bond formed through the mixing of $d_{z2}(Ti)$ and $p_z(N)$, two π bonds ($d_{xz}(Ti)+p_x(N)$ and $d_{yz}(Ti)+p_y(N)$) polarized toward N, and a lone pair at the nitride center (n(N) in Figure 5) with spatial characteristics of the 2s(N) orbital.[50]

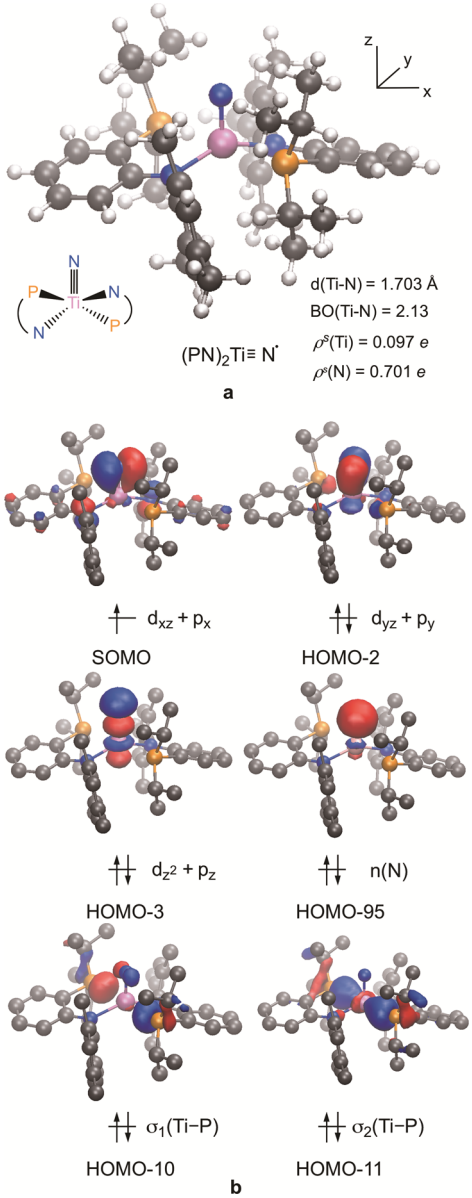

Figure 5. Relevant QROs of the nitridyl **A** characterizing Ti−N bonding, lone pair at N and Ti−P bonds.

The QROs selected for display in Figure 5 clearly reveal these σ (HOMO−3) and π type (SOMO and HOMO−2) titanium−nitrogen interactions in **A**. Moreover, the singly occupied orbital (SOMO) corresponds to the π bond of the $d_{xz}(Ti)+p_x(N)$ combination and, accordingly, it illustrates the π nature of the radical in **A**. As this orbital is greatly polarized toward the nitrogen, it is formally characterized as a nitridyl radical, which is also corroborated by the atomic spin densities of 0.7 at N and 0.1 at Ti. This half-filled orbital also accounts for the increased Ti−N distance (1.70 Å vs 1.66 Å) and reduced bond order (2.13 vs 2.54) in **A** with respect to the nitride species $[(PN)_2Ti{\equiv}N]^-$. Namely, when going from the titanium-nitridyl to the titanium-nitride, this half-filled orbital gets populated and, since it is a bonding combination, the Ti−

https://doi.org/10.1021/acs.inorgchem.0c03644
Inorg. Chem. 2021, 60, 5635−5646

N interaction becomes stronger, which is manifested in the shortening of the bond and larger bond index. Finally, the π nature of the radical at N plausibly plays a role in the observed reactivity of this nitridyl complex; it explains its facile insertion into the Ti−P bond, characterized by a low activation barrier of 16.2 kcal mol^{-1} in solution state. As a matter of fact, solvation has a prominent destabilization effect on the transition state and, accordingly, the activation Gibbs free energy corresponding to the insertion of the nitridyl center into the Ti−P bond is only 5.86 kcal mol^{-1} in the gas phase at 20 K, which is a more realistic simulation when compared to the frozen matrix conditions at which our EPR spectroscopic study had been conducted.

CONCLUSIONS

In this study, we have investigated the chemistry of an elusive, electron deficient nitride of titanium. Although our synthetic and spectroscopic studies have not allowed for the direct observation of a transient titanium nitridyl, **A**, we have shown how two independent routes can result in chemistry suggestive of an electrophilic nitride and how such reactive functionality can oxidize a phosphino group to the phosphinimide-halide complexes **2** and **3**. By oxidizing a Ti(IV) nitride anion **1**, the unstable nitridyl moiety can engage in phosphine oxidation competitively with H atom abstraction to form the parent imide, **4**. Control reactions have demonstrated how **4** can be photochemically active and undergo imide transfer to the phosphine concurrent with formation of a titanium-hydride, **5**. We have also showed how nitridyl species **A** can be *in situ* generated photochemically by azide fragmentation of complex **6** to N_2 and **4**, the latter of which can react further to produce **5**. Attempts to spectroscopically observe **A** via frozen matrix photochemical reactivity of **5** resulted instead in nitridyl insertion into the phosphine group, as opposed to HAT commonly observed in solution phase conditions. Theoretical studies have been conducted in order to understand how the unstable nitridyl in **A** (or imide in **4**) can oxidize the phosphine moiety and that such a process is essentially barrierless. Likewise, theoretical studies also allowed us to gain an appreciation for the electronic structure of radical **A** and demonstrated this square pyramidal species to possess a Ti−$N_{nitridyl}$ bond order of 2.1 (hence longer Ti−N distance when compared to **1**). Atomic spin densities clearly show the radical to be nitrogen centric and in accord with this moiety being quite oxidizing and elusive even under frozen matrix conditions.

ASSOCIATED CONTENT

Supporting Information

The Supporting Information is available free of charge at https://pubs.acs.org/doi/10.1021/acs.inorgchem.0c03644.

Experimental procedures, spectral data, and computational details (PDF)

Accession Codes

CCDC 1967031−1967033 contain the supplementary crystallographic data for this paper. These data can be obtained free of charge via www.ccdc.cam.ac.uk/data_request/cif, or by emailing data_request@ccdc.cam.ac.uk, or by contacting The Cambridge Crystallographic Data Centre, 12 Union Road, Cambridge CB2 1EZ, UK; fax: +44 1223 336033.

AUTHOR INFORMATION

Corresponding Authors

Balazs Pinter − *Department of Chemistry, Universidad Técnica Federico Santa María, Valparaíso 2390123, Chile;* orcid.org/0000-0002-0051-5229; Email: pinter.balazs@gmail.com

Daniel J. Mindiola − *Department of Chemistry, University of Pennsylvania, Philadelphia, Pennsylvania 19104, United States;* orcid.org/0000-0001-8205-7868; Email: mindiola@sas.upenn.edu

Authors

Lauren N. Grant − *Department of Chemistry, University of Pennsylvania, Philadelphia, Pennsylvania 19104, United States*

Mrinal Bhunia − *Department of Chemistry, University of Pennsylvania, Philadelphia, Pennsylvania 19104, United States*

Christophe Rebreyend − *Department of Homogeneous Catalysis, Universiteit van Amsterdam, Faculty of Science, van 't Hoff Institute for Molecular Sciences, Postbus 94720, Amsterdam*

Maria E. Carroll − *Department of Chemistry, University of Pennsylvania, Philadelphia, Pennsylvania 19104, United States;* orcid.org/0000-0001-7714-596X

Patrick J. Carroll − *Department of Chemistry, University of Pennsylvania, Philadelphia, Pennsylvania 19104, United States*

Bas de Bruin − *Department of Homogeneous Catalysis, Universiteit van Amsterdam, Faculty of Science, van 't Hoff Institute for Molecular Sciences, Postbus 94720, Amsterdam;* orcid.org/0000-0002-3482-7669

Complete contact information is available at: https://pubs.acs.org/10.1021/acs.inorgchem.0c03644

Author Contributions

[$]L.N.G. and M.B. contributed equally to this work.

Notes

The authors declare no competing financial interest.

ACKNOWLEDGMENTS

For funding, we thank the University of Pennsylvania and the Chemical Sciences, Geosciences, and Biosciences Division, Office of Basic Energy Sciences, Office of Science, U.S. DOE (DEFG02-07ER15893 to D.J.M., synthesis and characterization). L.N.G. thanks NSF GRFP for funding. B.d.B. thanks the Netherland Organization for Scientific Research (NWO−CW VICI project 016.122.613) and the University of Amsterdam (Research Priority Area Sustainable Chemistry) for financial support. B.P. acknowledges Fondecyt for the financial (No. 1191563) and the Centro Cientifico Tecnologico (CCTVal) for the computational resources and technical support.

REFERENCES

(1) Dempsey, J. L.; Winkler, J. R.; Gray, H. B. Proton-Coupled Electron Flow in Protein Redox Machines. *Chem. Rev.* **2010**, *110*, 7024−7039.

(2) Meunier, B.; de Visser, S. P.; Shaik, S. Mechanism of Oxidation Reactions Catalyzed by Cytochrome P450 Enzymes. *Chem. Rev.* **2004**, *104*, 3947−3980.

(3) Huang, X.; Groves, J. T. Oxygen Activation and Radical Transformations in Heme Proteins and Metalloporphyrins. *Chem. Rev.* **2018**, *118*, 2491−2553.
(4) Suarez, A. I.; Lyaskovskyy, V.; Reek, J. N.; van der Vlugt, J.; de Bruin, B. Complexes with nitrogen-centered radical ligands: classification, spectroscopic features, reactivity, and catalytic applications. *Angew. Chem., Int. Ed.* **2013**, *52*, 12510−12529.
(5) Curley, J. J.; Cook, T. R.; Reece, S. Y.; Müller, P.; Cummins, C. C. Shining Light on Dinitrogen Cleavage: Structural Features, Redox Chemistry, and Photochemistry of the Key Intermediate Bridging Dinitrogen Complex. *J. Am. Chem. Soc.* **2008**, *130*, 9394−9405.
(6) Tsai, Y.-C.; Cummins, C. C. Base-catalyzed dinitrogen cleavage by molybdenum amides. *Inorg. Chim. Acta* **2003**, *345*, 63−69.
(7) Mindiola, D. J.; Meyer, K.; Cherry, J.-P. F.; Baker, T. A.; Cummins, C. C. Dinitrogen Cleavage Stemming from a Heterodinuclear Niobium/Molybdenum N_2 Complex: New Nitridoniobium Systems Including a Niobazene Cyclic Trimer. *Organometallics* **2000**, *19*, 1622−1624.
(8) Laplaza, C. E.; Johnson, M. J. A.; Peters, J. C.; Odom, A. L.; Kim, E.; Cummins, C. C.; George, G. N.; Pickering, I. J. Dinitrogen Cleavage by Three-Coordinate Molybdenum(III) Complexes: Mechanistic and Structural Data. *J. Am. Chem. Soc.* **1996**, *118*, 8623−8638.
(9) Laplaza, C. E.; Johnson, A. R.; Cummins, C. C. Nitrogen Atom Transfer Coupled with Dinitrogen Cleavage and Mo−Mo Triple Bond Formation. *J. Am. Chem. Soc.* **1996**, *118*, 709−710.
(10) Laplaza, C. E.; Cummins, C. C. Dinitrogen Cleavage by a Three-Coordinate Molybdenum(III) Complex. *Science* **1995**, *268*, 861−863.
(11) Morello, L.; Yu, P.; Carmichael, C. D.; Patrick, B. O.; Fryzuk, M. D. Formation of Phosphorus-Nitrogen Bonds by Reduction of a Titanium Phosphine Complex under Molecular Nitrogen. *J. Am. Chem. Soc.* **2005**, *127*, 12796−12797.
(12) Fajardo, J., Jr.; Peters, J. C. Catalytic Nitrogen-to-Ammonia Conversion by Osmium and Ruthenium Complexes. *J. Am. Chem. Soc.* **2017**, *139*, 16105−16108.
(13) Buscagan, T. M.; Oyala, P. H.; Peters, J. C. N_2-to-NH_3 Conversion by a triphos-Iron Catalyst and Enhanced Turnover under Photolysis. *Angew. Chem., Int. Ed.* **2017**, *56*, 6921−6926.
(14) Rittle, J.; Peters, J. C. An Fe-N_2 Complex That Generates Hydrazine and Ammonia via Fe=NNH_2: Demonstrating a Hybrid Distal-to-Alternating Pathway for N_2 Reduction. *J. Am. Chem. Soc.* **2016**, *138*, 4243−4248.
(15) MacLeod, K. C.; Holland, P. L. Recent developments in the homogeneous reduction of dinitrogen by molybdenum and iron. *Nat. Chem.* **2013**, *5*, 559−565.
(16) MacLeod, K. C.; McWilliams, S. F.; Mercado, B. Q.; Holland, P. L. Stepwise N−H bond formation from N_2-derived iron nitride, imide and amide intermediates to ammonia. *Chem. Sci.* **2016**, *7*, 5736−5746.
(17) MacLeod, K. C.; Vinyard, D. J.; Holland, P. L. A Multi-iron System Capable of Rapid N_2 Formation and N_2 Cleavage. *J. Am. Chem. Soc.* **2014**, *136*, 10226−10229.
(18) Rodriguez, M. M.; Bill, E.; Brennessel, W. W.; Holland, P. L. N_2 Reduction and Hydrogenation to Ammonia by a Molecular Iron-Potassium Complex. *Science* **2011**, *334*, 780−783.
(19) Abbenseth, J.; Finger, M.; Würtele, C.; Kasanmascheff, M.; Schneider, S. Coupling of terminal iridium nitrido complexes. *Inorg. Chem. Front.* **2016**, *3*, 469−477.
(20) Scheibel, M. G.; Wu, Y.; Stückl, A. C.; Krause, L.; Carl, E.; Stalke, D.; de Bruin, B.; Schneider, S. Synthesis and Reactivity of a Transient, Terminal Nitrido Complex of Rhodium. *J. Am. Chem. Soc.* **2013**, *135*, 17719−17722.
(21) Brown, S. N. Insertion of a Metal Nitride into Carbon−Carbon Double Bonds. *J. Am. Chem. Soc.* **1999**, *121*, 9752−9753.
(22) Brown, S. N. Oxidative Azavinylidene Formation in the Reaction of 1,3-Diphenylisobenzofuran with Osmium Nitride Complexes. *Inorg. Chem.* **2000**, *39*, 378−381.
(23) Maestri, A. G.; Cherry, K. S.; Toboni, J. J.; Brown, S. N. [4 + 1] Cycloadditions of Cyclohexadienes with Osmium Nitrides. *J. Am. Chem. Soc.* **2001**, *123*, 7459−7460.
(24) Seymore, S. B.; Brown, S. N. Polar Effects in Nitride Coupling Reactions. *Inorg. Chem.* **2002**, *41*, 462−469.
(25) Maestri, A. G.; Taylor, S. D.; Schuck, S. M.; Brown, S. N. Cleavage of Conjugated Alkenes by Cationic Osmium Nitrides: Scope of the Reaction and Dynamics of the Azaallenium Products. *Organometallics* **2004**, *23*, 1932−1946.
(26) Schendzielorz, F. S.; Finger, M.; Volkmann, C.; Würtele, C.; Schneider, S. A Terminal Osmium(IV) Nitride: Ammonia Formation and Ambiphilic Reactivity. *Angew. Chem., Int. Ed.* **2016**, *55*, 11417−11420.
(27) Scheibel, M. G.; Abbenseth, J.; Kinauer, M.; Heinemann, F. W.; Würtele, C.; de Bruin, B.; Schneider, S. Homolytic N−H Activation of Ammonia: Hydrogen Transfer of Parent Iridium Ammine, Amide, Imide, and Nitride Species. *Inorg. Chem.* **2015**, *54*, 9290−9302.
(28) Schrock, R. R. Catalytic Reduction of Dinitrogen to Ammonia at a Single Molybdenum Center. *Acc. Chem. Res.* **2005**, *38*, 955−962.
(29) Tran, B. L.; Washington, M.; Henckel, D. A.; Gao, X.; Pink, M.; Mindiola, D. J. A four coordinate parent imidevia a titanium nitridyl. *Chem. Commun.* **2012**, *48*, 1529−1531.
(30) Thompson, R.; Wu, G.; Chen, C.-H.; Pink, M.; Mindiola, D. J. A Nitrido Salt Reagent of Titanium. *J. Am. Chem. Soc.* **2014**, *136*, 8197−8200.
(31) Grant, L. N.; Pinter, B.; Gu, J.; Mindiola, D. J. Molecular Zirconium Nitride Super Base from a Mononuclear Parent Imide. *J. Am. Chem. Soc.* **2018**, *140*, 17399−17403.
(32) Cowley, R. E.; Holland, P. L. Ligand Effects on Hydrogen Atom Transfer from Hydrocarbons to Three-Coordinate Iron Imides. *Inorg. Chem.* **2012**, *51*, 8352−8361.
(33) Kogut, E.; Wiencko, H. L.; Zhang, L.; Cordeau, D. E.; Warren, T. H. A Terminal Ni(III)−Imide with Diverse Reactivity Pathways. *J. Am. Chem. Soc.* **2005**, *127*, 11248−11249.
(34) Cowley, R. E.; Eckert, N. A.; Vaddadi, S.; Figg, T. M.; Cundari, T. R.; Holland, P. L. Selectivity and Mechanism of Hydrogen Atom Transfer by an Isolable Imidoiron(III) Complex. *J. Am. Chem. Soc.* **2011**, *133*, 9796−9811.
(35) Hennessy, E. T.; Betley, T. A. Complex N-Heterocycle Synthesis via Iron-Catalyzed, Direct C−H Bond Amination. *Science* **2013**, *340*, 591−595.
(36) A nitridyl or radical of cobalt has been proposed to engage in C−H insertion chemistry. Atienza, C. C. H.; Bowman, A. C.; Lobkovsky, E.; Chirik, P. J. Photolysis and Thermolysis of Bis(imino)pyridine Cobalt Azides: C−H Activation from Putative Cobalt Nitrido Complexes. *J. Am. Chem. Soc.* **2010**, *132*, 16343−16345.
(37) Wiese, S.; McAfee, J. L.; Pahls, D. R.; McMullin, C. L.; Cundari, T. R.; Warren, T. H. C−H Functionalization Reactivity of a Nickel−Imide. *J. Am. Chem. Soc.* **2012**, *134*, 10114−10121.
(38) Badiei, Y. M.; Dinescu, A.; Dai, X.; Palomino, R. M.; Heinemann, F. W.; Cundari, T. R.; Warren, T. H. Copper-nitrene complexes in catalytic C-H amination. *Angew. Chem., Int. Ed.* **2008**, *47*, 9961−9964.
(39) Aguila, M. J. B.; Badiei, Y. M.; Warren, T. H. Mechanistic Insights into C−H Amination via Dicopper Nitrenes. *J. Am. Chem. Soc.* **2013**, *135*, 9399−9406.
(40) Gephart, R. T.; Warren, T. H. Copper-Catalyzed sp^3 C−H Amination. *Organometallics* **2012**, *31*, 7728−7752.
(41) Gephart, R. T., III; Huang, D. L.; Aguila, M. J. B.; Schmidt, G.; Shahu, A.; Warren, T. H. Catalytic C-H Amination with Aromatic Amines. *Angew. Chem., Int. Ed.* **2012**, *51*, 6488−6492.
(42) Wiese, S.; Aguila, M. J. B.; Kogut, E.; Warren, T. H. *β*-Diketiminato Nickel Imides in Catalytic Nitrene Transfer to Isocyanides. *Organometallics* **2013**, *32*, 2300−2308.
(43) Scheibel, M. G.; Askevold, B.; Heinemann, F. W.; Reijerse, E. J.; de Bruin, B.; Schneider, S. Closed-shell and open-shell square-planar iridium nitrido complexes. *Nat. Chem.* **2012**, *4*, 552−558.

https://doi.org/10.1021/acs.inorgchem.0c03644
Inorg. Chem. 2021, 60, 5635−5646

(44) Gloaguen, Y.; Rebreyend, C.; Lutz, M.; Kumar, P.; Huber, M.; van der Vlugt, I. J. I.; Schneider, S.; de Bruin, B. An Isolated Nitridyl Radical-Bridged {Rh($N^{\bullet}$)Rh} Complex. *Angew. Chem., Int. Ed.* **2014**, *53*, 6814−6818.
(45) Meyer, K.; Bill, E.; Mienert, B.; Weyhermuller, T.; Wieghardt, K. Photolysis of cis- and trans-$[Fe^{III}(cyclam)(N_3)_2]^+$ Complexes: Spectroscopic Characterization of a Nitridoiron(V) Species. *J. Am. Chem. Soc.* **1999**, *121*, 4859−4876.
(46) Grapperhaus, C. A.; Mienert, B.; Bill, E.; Weyhermuller, T.; Wieghardt, K. Mononuclear (Nitrido)iron(V) and (Oxo)iron(IV) Complexes via Photolysis of $[(cyclam\text{-}acetato)Fe^{III}(N_3)]^+$ and Ozonolysis of $[(cyclam\text{-}acetato)Fe^{III}(O_3SCF_3)]^+$ in Water/Acetone Mixtures. *Inorg. Chem.* **2000**, *39*, 5306−5317.
(47) Grubel, K.; Brennessel, W. W.; Mercado, B. Q.; Holland, P. L. Alkali Metal Control over N−N Cleavage in Iron Complexes. *J. Am. Chem. Soc.* **2014**, *136*, 16807−16816.
(48) Vreeken, V.; Baij, L.; de Bruin, B.; Siegler, M. A.; van der Vlugt, J. I. N-Atom transfer via thermal or photolytic activation of a Co-azido complex with a PNP pincer ligand. *Dalton Trans.* **2017**, *46*, 7145−7149.
(49) Carroll, M. E.; Pinter, B.; Carroll, P. J.; Mindiola, D. J. Mononuclear and Terminally Bound Titanium Nitrides. *J. Am. Chem. Soc.* **2015**, *137*, 8884−8887.
(50) Grant, L. N.; Pinter, B.; Kurogi, T.; Carroll, M. E.; Wu, G.; Manor, B. C.; Carroll, P. J.; Mindiola, D. J. Molecular titanium nitrides: nucleophiles unleashed. *Chem. Sci.* **2017**, *8*, 1209−1224.
(51) Inside the nitrogen filled glovebox, J. young NMR tube (NT 1) was charged with dimer **1** (38 mg, 0.02 mmol), I_2 (10.2 mg, 0.04 mmol), and C_6D_6 (0.6 mL) and connected through a bridgehead connector with another J. young NMR tube (NT 2) loaded with styrene (0.1 mmol) and Pd/C (55 mg) in THF (1.0 mL). Then the NMR tube (NT 2) was degassed, kept in static vacuum, and the other NMR tube (NT 1) was charged with UV light (360 nm) for 15 min. The evolved hydrogen gas in NT 1 NMR tube could transfer to other NMR tube (NT 2) loaded with styrene and Pd/charcoal, while the NT 2 was dipped in liquid N_2 to allow the transfer of evolved hydrogen gas. Next, we warmed the bridgehead connector to make sure the transfer of maximum evolved hydrogen gas and after tightening of NT 2, it was warmed to room temperature and then placed in a preheated oil bath at 120 °C for overnight. ^1H NMR spectroscopy of the reaction mixture in $CDCl_3$ suggests 7% reduction of styrene to ethylbenzene, which indicates one equiv dimer produced roughly 0.35 equiv of H_2.
(52) Addison, A. W.; Rao, T. N.; Reedijk, J.; van Rijn, J.; Verschoor, G. C. Synthesis, structure, and spectroscopic properties of copper(II) compounds containing nitrogen−sulphur donor ligands; the crystal and molecular structure of aqua[1,7-bis(N-methylbenzimidazol-2′-yl)-2,6-dithiaheptane]copper(II) perchlorate. *J. Chem. Soc., Dalton Trans.* **1984**, 1349−1356.
(53) Moret, M.-E.; Peters, J. C. N_2 Functionalization at Iron Metallaboratranes. *J. Am. Chem. Soc.* **2011**, *133*, 18118−18121.
(54) Lin, H.-J.; Siretanu, D.; Dickie, D. A.; Subedi, D.; Scepaniak, J. J.; Mitcov, D.; Clérac, R.; Smith, J. M. Steric and Electronic Control of the Spin State in Three-Fold Symmetric, Four-Coordinate Iron(II) Complexes. *J. Am. Chem. Soc.* **2014**, *136*, 13326−13332.
(55) Scepaniak, J. J.; Harris, T. D.; Vogel, C. S.; Sutter, J.; Meyer, K.; Smith, J. M. Spin Crossover in a Four-Coordinate Iron(II) Complex. *J. Am. Chem. Soc.* **2011**, *133*, 3824−3827.
(56) Scepaniak, J. J.; Fulton, M. D.; Bontchev, R. P.; Duesler, E. N.; Kirk, M. L.; Smith, J. M. Structural and Spectroscopic Characterization of an Electrophilic Iron Nitrido Complex. *J. Am. Chem. Soc.* **2008**, *130*, 10515−10517.
(57) Buschhorn, D.; Pink, M.; Fan, H.; Caulton, K. G. Nitrogen-Ligated Iron Complexes: Photolytic Approach to the FeN^+ Moiety. *Inorg. Chem.* **2008**, *47*, 5129−5135.
(58) Adhikari, D.; Basuli, F.; Fan, H.; Huffman, J. C.; Pink, M.; Mindiola, D. J. P=N Bond Formation via Incomplete N-Atom Transfer from a Ferrous Amide Precursor. *Inorg. Chem.* **2008**, *47*, 4439−4441.
(59) de Wolf, J. M.; Meetsma, A.; Teuben, J. H. Synthesis and Structure of Bis(phenyltetramethylcyclopentadienyl)titanium(III) Hydride: First Monomeric Bis(cyclopentadienyl)titanium(III) Hydride. *Organometallics* **1995**, *14*, 5466−5468.
(60) Pez, G. P.; Kwan, S. C. Chemistry of.mu.-(.eta.1:.eta.5-cyclopentadienyl)-tris(.eta.-cyclopentadienyl)dititanium(Ti-Ti). 2. Reactivity with hydrogen and nitrogen and catalytic properties. *J. Am. Chem. Soc.* **1976**, *98*, 8079−8083.
(61) Pattiasina, J. W.; van Bolhuis, F.; Teuben, J. H. Titanium Hydride Formation through Hydrogen Transfer from 2-Methylpyridine to a Titanium Fulvene Compound; the First Structurally Characterized Terminal Titanium Hydride. *Angew. Chem., Int. Ed. Engl.* **1987**, *26*, 330−331.
(62) Luinstra, G. A.; Teuben, J. H.; Brintzinger, H.-H. IR studies at elevated gas pressures III. Kinetics of the CO induced disproportionation of $(C_5(CH_3)_5)_2TiX$ (X = Cl, Br, I). *J. Organomet. Chem.* **1989**, *375*, 183−190.
(63) Ma, K.; Piers, W. E.; Gao, Y.; Parvez, M. Isolation and characterization of a monomeric cationic titanium hydride. *J. Am. Chem. Soc.* **2004**, *126*, 5668−5669.
(64) Gomberg, M. An Instance of Trivalent Carbon: Triphenylmethyl. *J. Am. Chem. Soc.* **1900**, *22*, 757−771.
(65) On the basis of TD-DFT studies, it can be concluded that N_2 loss from **6** does not originate from an excited state in which electrons of Ti-P interaction promotes azide reduction without invoking a transient titanium nitridyl (see SI for details).
(66) Grant, L. N.; Krzystek, J.; Ozarowski, A.; Telser, J.; Grützmacher, H.; Mindiola, D. J. Finding a soft spot for vanadium: A P-bound OCP ligand. *Chem. Commun.* **2019**, *55*, 5966−5969.

https://doi.org/10.1021/acs.inorgchem.0c03644
Inorg. Chem. 2021, 60, 5635−5646